ACADEMIC PRESS

Available online at www.sciencedirect.com

SCIENCE DIRECT®

Journal of Sound and Vibration 265 (2003) 609–625

JOURNAL OF SOUND AND VIBRATION

www.elsevier.com/locate/jsvi

Identification of modal parameters including unmeasured forces and transient effects

B. Cauberghe*, P. Guillaume, P. Verboven, E. Parloo

Department of Mechanical Engineering, Vrije Universiteit Brussel, Pleinlaan 2, B-1050 Brussels, Belgium

Received 26 April 2002; accepted 25 July 2002

Abstract

In this paper, a frequency-domain method to estimate modal parameters from short data records with known input (measured) forces and unknown input forces is presented. The method can be used for an experimental modal analysis, an operational modal analysis (output-only data) and the combination of both. A traditional experimental and operational modal analysis in the frequency domain starts respectively, from frequency response functions and spectral density functions. To estimate these functions accurately sufficient data have to be available. The technique developed in this paper estimates the modal parameters directly from the Fourier spectra of the outputs and the known input. Instead of using Hanning windows on these short data records the transient effects are estimated simultaneously with the modal parameters. The method is illustrated, tested and validated by Monte Carlo simulations and experiments. The presented method to process short data sequences leads to unbiased estimates with a small variance in comparison to the more traditional approaches.

1. Introduction

In the past different methods were developed to process output-only data [1]. These methods can be used for situations where it is difficult to perform an artificial forced excitation. The main idea of the output-only modal analysis is to use the unknown natural forces as excitation (e.g., traffic/wind excitation for civil structures, atmospheric turbulence for airplanes, etc.). A benefit of an operational modal analysis is that the modal parameters are identified in real operational conditions, which can differ a lot with laboratory conditions.

*Corresponding author. Tel.: +2-629-2805; fax: +2-629-2865.
E-mail address: bart.cauberghe@vub.ac.be (B. Cauberghe).

0022-460X/03/$ - see front matter
doi:10.1016/S0022-460X(02)01526-2

An experimental modal analysis starts from input and output measurements to estimate the modal parameters. In this case all natural unknown forces are considered as undesirable process noise on the output measurements. The use of a non-parametric H_1 frequency response function (FRF) estimator eliminates the noise contributions on the outputs. When sufficient data samples are available the FRFs can be estimated without suffering from a low-frequency resolution. Recently, maximum likelihood (MLE FRF) estimators were developed to deal with noisy FRF data [2].

A bridge excited with a shaker but on the same time by the traffic, or flight flutter tests where the airplane is excited by its flaps but on the same time by atmospheric turbulence, are practical examples in which the structure is excited with a known force but at the same time with unknown forces. Traditional methods such as the least squares complex exponential (LSCE), least squares complex frequency domain (LSCF), or MLE estimators can only handle this problem if sufficient data is available because they start from FRFs [2]. Aircraft in-flight test data are typically characterized by short time records and a high noise level due to atmospheric turbulence. It is desired to decrease the flight flutter testing time for practical, economical and safety reasons and to improve the accuracy of the estimation [3–6]. Furthermore, to identify slow time-varying systems (e.g., a car at different speeds or under different road conditions, an airplane in different flight conditions) short time records, which, when small enough, can be assumed time invariant, must be processed. These examples show the need to develop methods which can deal with short time records and a combination of known and unknown input forces.

2. Theoretical aspects

The considered situation is represented in Fig. 1 with F the known input spectra (consider only one known input for reasons of simplicity), E_i the unknown white-noise input spectra, n_o^Y the

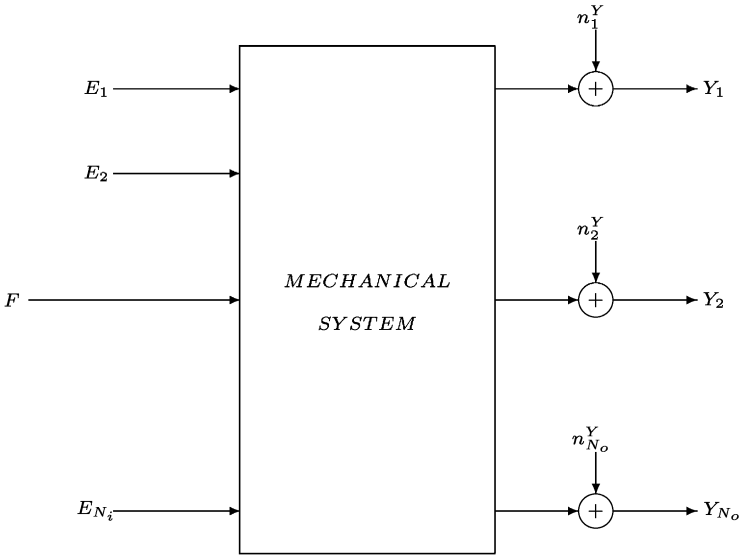

Fig. 1. Frequency-domain errors-in-variables noise model.

noise on the outputs and Y_o the measured output spectra. If the known input F is zero, the scheme represents an operational modal analysis. Relationship (1) between the discrete signals can be written as

$$\{\mathbf{y}(t)\} = \{\mathbf{H}(q,\theta)\}f(t) + [\mathbf{G}(q,\eta)]\{\mathbf{e}(t)\}, \quad t = 0, 1, \ldots, N-1, \tag{1}$$

with $\dim(\{\mathbf{H}(q,\theta)\}) = N_o \times 1$, $\dim([\mathbf{G}(q,\eta)]) = N_o \times N_i$, N_o the number of outputs and N_i the number of unknown inputs. Since $\{\mathbf{H}(q,\theta)\}$ and $[\mathbf{G}(q,\eta)]$ represent the same mechanical system, they have the same physical poles.

2.1. Experimental modal analysis

The process noise $[\mathbf{G}(q,\eta)]\{\mathbf{e}(t)\}$ is considered as undesirable noise on the output in a traditional modal analysis. The use of the H_1 non-parametric estimation of the FRFs eliminates this noise contribution (as a result the information contained in $[\mathbf{G}]$ is not used) under the assumption that $\{\mathbf{e}(t)\}$ is uncorrelated with $f(t)$, thus

$$\{\mathbf{H}\}_1 = \frac{\sum_{n=1}^{M}\{\mathbf{Y}\}_n F_n^*}{\sum_{n=1}^{M} F_n F_n^*}, \tag{2}$$

with M being the number of averages. Enough averaging yields to an accurate estimation of the FRFs if there is no noise on the inputs. A maximum likelihood estimator can work with less averages and as a consequence more noise on the FRFs, but still a minimum number of averages (typically 4) is necessary to obtain the noise information. All FRF-based estimators deal with a trade-off in an effort to produce statistically reliable spectral estimates (i.e., minimize the variances by increasing M) of a highest possible frequency resolution (i.e., maximize the number of samples within the record) from a finite amount of data samples [7]. If no periodic signals are used, leakage problems appear in the case of short data sequences. The use of a window—such as for instance a Hanning window—certainly helps to reduce the effects of leakage, but introduces a bias error. One concludes that methods based on an averaging process need sufficient data to keep a reasonable frequency resolution and to deal with process noise and leakage.

2.2. Operational modal analysis

If the known input F is zero, Fig. 1 represents an operational modal analysis. Frequency-domain output-only methods start from the power- and cross-spectral densities of the output measurements $[\mathbf{S}_{yy}(\mathrm{j}\omega)] = 1/N \sum_{n=1}^{N} Y_n Y_n^{\mathrm{H}}$ to estimate the modal parameters. The frequency-domain methods are based on Eq. (3), which holds for stationary stochastic processes

$$[\mathbf{S}_{yy}(\mathrm{j}\omega)] = [\mathbf{H}(\mathrm{j}\omega)][\mathbf{S}_{ee}(\mathrm{j}\omega)][\mathbf{H}(\mathrm{j}\omega)]^{\mathrm{H}}. \tag{3}$$

In case of white-noise inputs, the density matrix of the inputs $[\mathbf{S}_{ff}(\mathrm{j}\omega)]$, is a constant matrix independent of the frequency. According to the modal theory, the FRF matrix $[\mathbf{H}(\mathrm{j}\omega)]$ can be decomposed as

$$[\mathbf{H}(\mathrm{j}\omega)] = \sum_{r=1}^{N_m}\left(\frac{\{\boldsymbol{\psi}_r\}\{\mathbf{L}_r\}^{\mathrm{T}}}{\mathrm{j}\omega - \lambda_r} + \frac{\{\boldsymbol{\psi}_r\}^*\{\mathbf{L}_r\}^{\mathrm{H}}}{\mathrm{j}\omega - \lambda_r^*}\right). \tag{4}$$

where N_m is the number of modes, λ_r is the rth pole, $\{\psi_r\}$ is the rth mode shape and $\{\mathbf{L}_r\}$ is the participation vector of the rth mode. Substituting Eq. (4) into Eq. (3) and assuming white-noise inputs leads to

$$[\mathbf{S}_{yy}(\mathrm{j}\omega)] = \sum_{r=1}^{N_m} \left(\frac{\{\psi_r\}\{\mathbf{Q}_r\}^{\mathrm{T}}}{\mathrm{j}\omega - \lambda_r} + \frac{\{\psi_r\}^{*}\{\mathbf{Q}_r\}^{\mathrm{H}}}{\mathrm{j}\omega - \lambda_r^{*}} + \frac{\{\mathbf{Q}_r\}\{\psi_r\}^{\mathrm{T}}}{-\mathrm{j}\omega - \lambda_r} + \frac{\{\mathbf{Q}_r\}^{*}\{\psi_r\}^{\mathrm{H}}}{-\mathrm{j}\omega - \lambda_r^{*}} \right). \tag{5}$$

The reference vector $\{\mathbf{Q}_r\}$ of the rth mode depends on the constant $[\mathbf{S}_{ff}]$ matrix and the modal parameters of the structure. Eq. (5) forms the basis to extract the modal parameters from the frequency-domain output-only data. One of the drawbacks of these methods is that sufficient data have to be available to perform an accurate non-parametric estimation of the power- and cross-spectral density functions of the output measurements. Two methods exist to estimate these spectral density functions [8]. The direct method, periodogram method, divides the time-domain data in different blocks which are transferred to the frequency domain and averaged. Typically, Hanning windows are used to reduce the leakage of these short data blocks. The indirect method first estimates the auto- and cross-correlation to obtain the spectral density by Fourier transforming these time functions to the frequency domain. Both approaches have to make a trade-off between the variance and bias of the non-parametric estimation (e.g., the direct method applied on many short data blocks leads to a small variance, but a larger bias error due to leakage). Again one concludes that enough data has to be available to use the classical spectral density approach to process output-only measurements.

2.3. Combined operational–experimental modal analysis

In the previous two subsections a contradiction clearly appears: in the case of an experimental modal analysis the process noise $[\mathbf{G}(q,\eta)]\{\mathbf{e}(t)\}$ is considered as undesirable, where in the operational modal analysis this information is used to obtain the modal parameters. An estimation based on the frequency spectra of the outputs and the known inputs leads to an approach where all the information is used. In this section a combined non-linear least squares frequency method on input output spectra (CLSF-IO) is proposed.

This approach can deal with short time data records, since no averaging process is used and hence the spectra of the total time record is used, which leads to a higher frequency resolution. A scalar representation of Eq. (6) in the discrete frequency domain yields

$$Y_o(k) = H_o(k,\theta)F(k) + \sum_{n=1}^{N_i} G_{oi}(k,\eta)E_i(k), \tag{6}$$

where $X_k = (1/\sqrt{N})\sum_{n=0}^{N-1} x(n)\mathrm{e}^{-\mathrm{i}2\pi nk/N}$ ($X = Y_o, F, E_i$ and $x = y_o, f, e_i$). Since $E_o(k)$ is assumed to be normal distributed white noise, the sum $\sum_{n=1}^{N_i} G_{oi}(k,\eta)E_i(k)$ can be replaced for each output by $G_o(k,\eta)E_o(k)$ with $E_o(k)$ a new normal distributed white noise source. Even when the unmeasured force $E_i(k)$ is not normally distributed, this substitution is valid by applying the central limit theorem [9]. In this way each output can be represented by

$$Y_o(k) = H_o(k,\theta)F(k) + G_o(k,\eta)E_o(k). \tag{7}$$

Using a common-denominator model leads to

$$Y_o(k) = \frac{A_o(z_k, a_o)}{B(z_k, b)} F(k) + \frac{C_o(z_k, c_o)}{B(z_k, b)} E_o(k) + \frac{T_o(z_k, t_o)}{B(z_k, b)}, \tag{8}$$

where $A_o(z_k, a_o), B_o(z_k, b_o), C_o(z_k, c_o)$ and $T_o(z_k, m_o)$ are polynomials in z_k with, respectively, coefficients $x = [x_1 x_2 \ldots x_{N_x}]$ $(x = a_o, c_o, b, t_o)$ and $z_k = \exp(\mathrm{j}2\pi k/N)$. $T_o(z_k, t_o) = \sum_{n=0}^{N_t} t_{on} z^n$ is a polynomial of order $N_t = \max(N_a, N_b, N_c) - 1$ $(N_a = N_c)$ that takes into account the transient effects caused by the finite length of the data [10]. The appearance of the extra polynomial $T_o(z_k, t_o)$ can be understood by considering the Laplace transform of the jth derivative of the force signal $f(t)$

$$L\left\{\frac{\mathrm{d}^j f(t)}{\mathrm{d}t^j} = s^j - \sum_{r=0}^{j-1-r} \frac{\mathrm{d}^r f(t)}{\mathrm{d}t^r}\right\}\Bigg|_{t=0}, \tag{9}$$

where the sum over the initial conditions introduces the polynomial. The use of a common denominator $B(z, b)$ for all outputs leads to global estimates of the poles. Since the denominators of $H_o(k, \theta)$ and $G_o(k, \eta)$ are modelled with the same polynomial $B(z, b)$ the information in $G_o(k, \eta)$ is also used to determine the poles. For example if one mode is not observable in $\{\mathbf{H}(k, \theta)\}$ because the excitation F took place in a node, this mode can still be detected if it is excited by the unknown noise forces.

The CLSF-IO method forces a parametric model on the input–output measurements in such a way that the residues $E_o(k)$ (in the present case the unmeasured forces) will be white noise. This approach is similar to the identification process of auto regressive moving average (ARMA) models in the time domain where the minimization of the prediction error $e(t)$ leads to the model parameters. This prediction error $e(t)$ of an ARMA process $m_0 y(t) + m_1 y(t-1) + \cdots + m_n y(t-n) = d_0 e(t) + d_1 e(t) + \cdots + d_k e(t-k)$ can be considered as an unknown excitation source. Thus the frequency-domain estimates of the parameters a, b, c and t are obtained by minimizing the cost function $V(a, b, v, t)$ Eq. (10) with respect to the parameters $a = [a_1, a_2, \ldots, a_{N_o}]$, $c = [c_1, c_2, \ldots, c_{N_o}]$ and $t = [t_1, t_2, \ldots, t_{N_o}]$:

$$V(a, b, c, t) = \sum_{o=1}^{N_o} V_o(a_o, c_o, b, t_o), \tag{10}$$

where

$$V_o(a_o, c_o, b, t_o) = \sum_{k=0}^{N_k - 1} |E_o(k, a_o, c_o, b, t_o)|^2,$$

$$E_o(k, a_o, c_o, b, t_o) = \frac{B(z_k, b) Y_o(k) - A_o(z_k, a_o) F(k) - T_o(z_k, t_o)}{C_o(z_k, c_o)},$$

with $N_k = N/2$. Because the expected value of every individual cost function $V_o(a_o, c_o, b, t_o)$ is minimal in the true parameters, the total cost function $V(a, b, c, t)$ is also minimal in the true parameters. Strong consistence follows under the assumption that $H_o(k, \theta)$ is a stable and inversely stable monic function and if the z_k values cover uniformly the unit circle $[0, 2\pi]$ in the case of complex coefficients and half the unit circle $[0, \pi]$ in case of real coefficients. Thus a scaling

of the frequency band of interest has to take place to fulfill this condition. A detailed discussion about the mathematical background and the different properties can be found in Refs. [9,11].

The poles of the structure are easily found by calculating the roots of $B(z,b)$. In case the unmeasured forces are not white, extra poles are identified which try to model the color of the unmeasured forces. The non-physical poles are characterized by a very high damping ratio and corresponding cancelling zeros in the deterministic part $H_o(k,\theta)F(k)$. The mode shapes are obtained from the residues of $\{\mathbf{H}(k,\theta)\}$.

$$\{\psi\}_r = \lim_{z\to z_r} \frac{\{\mathbf{A}(z,a)\}}{B(z,b)}(z-z_r), \tag{11}$$

with $\{\mathbf{A}(z,m)\} = [\mathbf{A}_1(z,m_1), \ldots, \mathbf{A}_{N_o}(z,m_{N_o})]^{\mathrm{T}}$. In the case of one known input these residues are equal to the mode shapes. When multiple known inputs are used, a single value decomposition (SVD) on the residue matrix of each pole leads to the mode shapes and participation vectors. In the operational case $Y_o(k) = [C_o(z_k,c_o)/B(z_k,b)]E_o(k) + T_o(z_k,t_o)/B(z_k,b)$ all the parameters b,c,t can still be obtained by minimizing the same cost function. No problem occurs in the determination of the poles, but the mode shape information has to be calculated from the density matrix $\mathbf{S}_{yy}$ according to Eq. (5). The leakage free representation of the $\mathbf{S}_{yy}$ is given by Eq. (12).

$$\mathrm{S}_{yy}(P_k)_{(i,j)} = \frac{C_i(z_k,c_i)C_j^*(z_k,c_j)}{|B(z_k,b)|^2}. \tag{12}$$

Unfortunately, the proposed estimation method has the restriction that the system must be inversely stable in order to converge. This means that the estimated zeros of the $C_o(z,c_o)$ must be stable or inside the unit circle. This restriction is forced in the implementation and leads to a loss of phase information of the estimated numerators $C_o(z_k,c_o)$. So only the magnitude is well estimated and as a result only the diagonal elements of the density matrix S_{yy} can be calculated correctly, because they are real-valued and thus independent of the phase. From the unit modal a_r scaling model [12] relationship $R_{ii,r} = |\psi_{i,r}|^2$ can be established, with

$$R_{ii,r} = \lim_{z\to z_r} \frac{|C_i(z,c_i)|^2}{|B(z,b)|^2}(z-z_r). \tag{13}$$

As a result, only the magnitude of the mode shapes can be obtained from $G_o(k,\eta)$.

One summarizes that the proposed method determines the poles from $B(z,b)$, the mode shapes from $A_o(z,a_o)/B(z,b)$ and the magnitude of the mode shapes from $C_o(z,c_o)/B(z,b)$. So the method can be used in case of an experimental (known force), an operational modal analysis (only unknown forces) and in the combination (known and unknown forces). In the case of an operational modal analysis only the magnitude of the mode shapes can be retrieved. The method needs no Hanning window to reduce leakage effects and no averaging process to preprocess the data. As a result it well suited to process short time records with transient effects.

2.4. Implemented algorithm

A Gauss–Newton method is used to solve the non-linear optimization problem. The highest order coefficients b_{N_b}, c_{o,N_c} of the polynomials $B(z,b) = \sum_{n=0}^{N_d} b_n z^n$ and $C_o(z_k,c_o) = \sum_{n=0}^{N_n} c_{o,n} z^n$ are set to one to make the other parameters identifiable. The normal equations (14), to estimate

real-valued coefficients, are formed explicitly to speed up the implementation [2].

$$\begin{bmatrix} R_1 & 0 & \cdots & S_1 \\ 0 & R_2 & & S_2 \\ \vdots & & \ddots & \vdots \\ S_1^{\mathrm{H}} & S_2^{\mathrm{H}} & \cdots & T \end{bmatrix} \begin{bmatrix} \Delta P_1 \\ \Delta P_2 \\ \vdots \\ \Delta b \end{bmatrix} = - \begin{bmatrix} V_1 \\ V_2 \\ \vdots \\ F \end{bmatrix} \tag{14}$$

with

$$R_o = Re\left(\left[\frac{\partial E_o(a_o, b, c_o, t_o)}{\partial(a_o, b_o, t_o)} \right]^{\mathrm{H}} \left[\frac{\partial E_o(a_o, b, c_o, t_o)}{\partial(a_o, c_o, t_o)} \right] \right),$$

$$S_o = Re\left(\left[\frac{\partial E_o(a_o, b, c_o, t_o)}{\partial(a_o, c_o, t_o)} \right]^{\mathrm{H}} \left[\frac{\partial E_o(a_o, b, c_o, t_o)}{\partial(b)} \right] \right),$$

$$V_o = Re\left(\left[\frac{\partial E_o(a_o, b, c_o, t_o)}{\partial(a_o, c_o, t_o)} \right]^{\mathrm{H}} E_o \right),$$

$$T = \sum_{o=1}^{N_o} Re\left(\left[\frac{\partial E_o(a_o, b, c_o, t_o)}{\partial(b)} \right]^{\mathrm{H}} \left[\frac{\partial E_o(a_o, b, c_o, t_o)}{\partial(b)} \right] \right),$$

$$F = \sum_{o=1}^{N_o} Re\left(\left[\frac{\partial E_o(a_o, b, c_o, t_o)}{\partial(b)} \right]^{\mathrm{H}} E_o \right), \qquad \Delta P_o = [\Delta a_o^{\mathrm{T}} \ \Delta c_o^{\mathrm{T}} \ \Delta t_o^{\mathrm{T}}]^{\mathrm{T}}. \tag{15}$$

Eliminating the ΔP_o and inserting Eq. (16) in the last equation of the matrix equation structure (14) gives Eq. (17),

$$\Delta P_o = -R_o^{-1}(S_o \Delta b + V_o), \tag{16}$$

$$\sum_{o=1}^{No} -S_o^{\mathrm{H}} R_o^{-1}(S_o \Delta b + V_o) + T\Delta b + F = 0. \tag{17}$$

Solving Eq. (17) gives the polynomial coefficients b of the common denominator $B(z, b)$. Inserting these coefficients in Eq. (16) provides the coefficients a_o of $A_o(z, a_o)$, c_o of $C_o(z, c_o)$ and the coefficients t_o of $T_o(z, t_o)$. In this way the estimation can work iteratively and converges, if in each step the zeros of the nominators $C_o(z, c_o)$ are forced in the unit circle. In case of an experimental or mixed experimental–operational modal analysis starting values for b, a and t are obtained from a linear least squares problem. The starting values for c are set equal to those of a. In the operational case the c coefficients are set to one and the other coefficients b and t are again obtained from a least squares estimation. In the next two sections the CLSF-IO method will be validated by means of simulations and experiments.

3. Simulations

Fig. 2 illustrates the discrete mechanical system of 7 degrees of freedom (d.o.f.s) used to simulate some measurements. The 7 natural frequencies are chosen between 1 and 12 Hz. A total

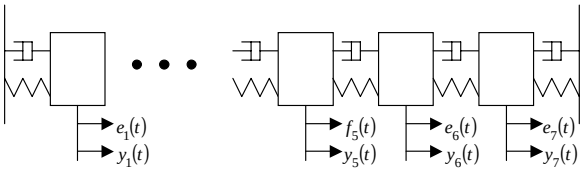

Fig. 2. Seven d.o.f. model.

measurement time of only 30 s was simulated while the system is excited by normal random noise (standard deviation $\sigma_{f(t)} = 1$) at location d.o.f. 5. Since the excitation signal is normal distributed noise, the output is also normally distributed. Two identification methods are compared to the CLSF-IO method. The first method is a frequency maximum likelihood estimator (MLE FRF), which starts from the FRFs. Minimizing the cost function (18) leads to an estimate of the modal parameters [2]

$$V(a,b,t)_{mle} = \sum_{o=1}^{N_o} \sum_{k=0}^{N_k-1} \frac{|A_o(z_k,a_o)/B(z_k,b) - H_o(z_k)|^2}{\mathrm{var}(H_o(k))}, \tag{18}$$

with $H_o(z_k)$ being the H_1 estimate of the FRF.

The second method is a maximum likelihood input–output (MLE-IO) method in the frequency domain [13]. This method minimizes the maximum likelihood cost function given by

$$V(m,d,t)_{mle} = \sum_{o=1}^{N_o} \sum_{k=0}^{N_k-1} \frac{|B(z_k,b)\,Y_o(k) - A_o(z_k,a_o)F(k) - T_o(z_k,t_o)|^2}{|B(z_k,b)|^2\,\mathrm{var}(Y_o(k))}, \tag{19}$$

where $\mathrm{var}(Y_o(k))$ can only be calculated by averaging the outputs in the case where a periodical excitation signal is used. In the case of an arbitrary input signal the variance $\mathrm{var}(Y_o(k))$ is set to one for each frequency and the MLE-IO reduces to a weighted non-linear least squares problem solved by a Newton–Gauss algorithm. While the CLSF-IO method estimates a parametric noise model, the MLE-IO uses a non-parametric noise model as a weighting.

To simulate a realistic situation independent measurement noise with $\sigma_n\{\mathbf{y}_o(t)\} = 0.04\sigma_{y_o(t)}$ is added to each output. Three different cases are simulated by solving the differential equations of the system: an experimental modal analysis; a combined experimental–operational analysis and an operational modal analysis. One hundred runs (for each run new noise sequences were generated to use as known input, unknown inputs and measurement noise on the outputs) of a Monte Carlo simulation is performed in each case. In each run of the Monte Carlo all three methods are used to identify the modal parameters. The natural frequencies and damping ratios are statistically processed. The mean value and the standard deviation of each natural frequency (m_f, σ_f) and damping ratio (m_d, σ_d) are compared to draw some conclusions. The availability of confidence intervals offered by MLE estimators must be taken with caution. The asymptotic properties of the MLE estimators cannot be used for these short data records and the full covariance matrix of the outputs should be taken into account in case of process noise (correlated noise over the different outputs).

3.1. Case I: experimental modal analysis

The simulated mechanical system is excited by one exactly known force $f(t)$ at d.o.f. 5 in the absence of unknown noise forces. For one run Fig. 3 shows the excitation signal (white noise) and the output at d.o.f. 6 in which the transient effect is still present. In each run the time record of Fig. 3 is divided in 4 equal time blocks to perform a H_1 estimate of the FRFs.

Table 1 gives an overview of the mean values and standard deviations of the natural frequencies and damping ratios over the different runs. It is clear that the MLE FRF, suffers from the low-frequency resolution, which yields to a high standard deviation on the natural frequency in comparison with the two other methods. The Hanning window, used to calculate the H_1 estimate, introduces a bias and a large standard deviation on the damping ratio. Using a uniform window instead of a Hanning window leads to useless FRFs due to the very short time records. On the level of the natural frequencies the MLE-IO performs well, but serious problems arise in the determination of the damping ratios of the last five modes. The MLE-IO method suffers from the noise on the output, because no noise information var($Y_o(k)$) has been taken into account. The CLSF-IO method leads to unbiased damping ratios and natural frequencies and standard deviations 10–20 times smaller than with the classical FRF approach. It is clear that if no noise information is available the CLSF-IO method gives the best results even in absence of external noise inputs (process noise) to process short time records. Fig. 4 illustrates the damping ratios estimated by the CLSF-IO method and the MLE FRF method in each run of the Monte Carlo simulation. The synthesized FRF H_{65} of one run is shown in Figs. 5 and 6.

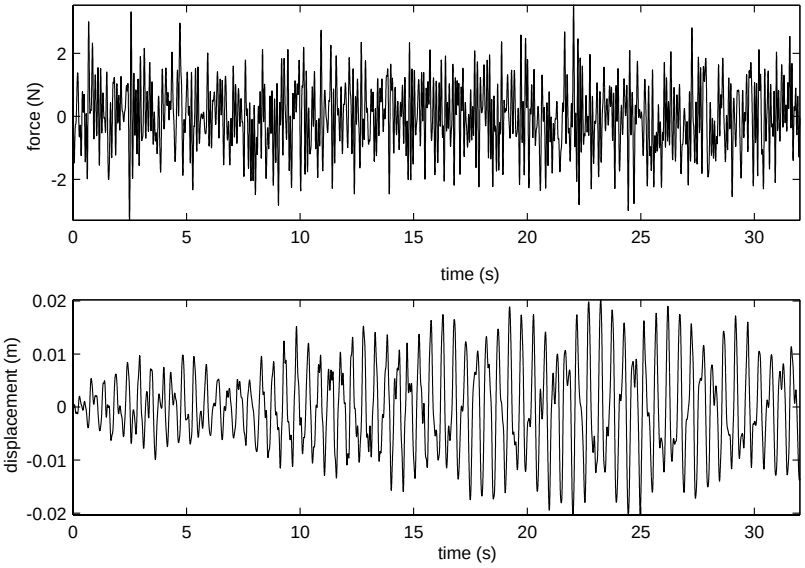

Fig. 3. Top, applied force $f(t)$ at d.o.f. 5; bottom, displacement of d.o.f. 6.

Table 1
Overview of modal parameter estimators—experimental approach

f_{exact} (Hz)	$m_{f\ CLSF-IO}$ (Hz)	$\sigma_{f\ CLSF-IO}$ (Hz)	$m_{f\ mle\ io}$ (Hz)	$\sigma_{f\ mle\ io}$ (Hz)	$m_{f\ mle\ frf}$ (Hz)	$\sigma_{f\ mle\ frf}$ (Hz)
2.02	2.02	1E-4	2.02	1E-4	2.02	0.043
3.72	3.72	2E-4	3.72	2E-4	3.71	0.026
5.45	5.45	0.001	5.45	0.010	5.46	0.027
6.80	6.80	0.000	6.80	0.001	6.80	0.016
8.39	8.39	0.003	8.37	0.025	8.39	0.024
9.19	9.19	0.002	9.20	0.010	9.19	0.020
10.52	10.53	0.004	10.52	0.007	10.52	0.017
d_{exact} (%)	$m_{d\ CLSF-IO}$ (%)	$\sigma_{d\ CLSF-IO}$ (%)	$m_{d\ mle\ io}$ (%)	$\sigma_{d\ mle\ io}$ (%)	$m_{d\ mle\ frf}$ (%)	$\sigma_{d\ mle\ frf}$ (%)
0.16	0.16	0.006	0.16	0.007	0.90	1.184
0.32	0.32	0.005	0.32	0.006	0.78	0.633
0.46	0.46	0.014	0.34	0.297	0.98	0.563
0.54	0.54	0.007	0.54	0.014	0.89	0.226
0.72	0.71	0.036	−0.02	0.784	1.11	0.491
0.68	0.68	0.020	0.56	0.26	1.06	0.239
0.95	0.94	0.035	0.80	0.243	1.27	0.160

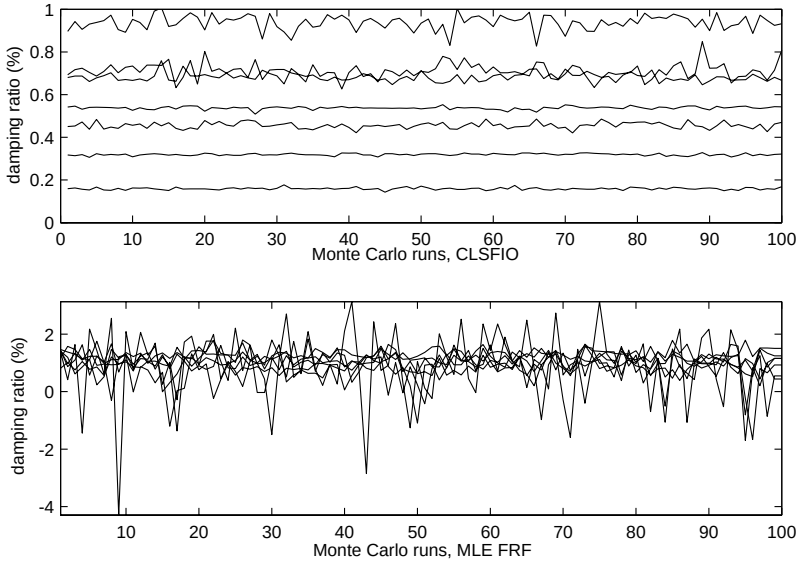

Fig. 4. Top, estimated damping ratios with the CLSF-IO method; bottom, estimated damping ratios with the MLE FRF method.

3.2. Case II: combined experimental–operational modal analysis

Besides the known force excitation in d.o.f. 5, the structure is also excited by unknown white noise ($\sigma_{e_i(t)} = 0.1\sigma_{f(t)}$) in the other d.o.f.s. The contribution in the outputs due to these unknown

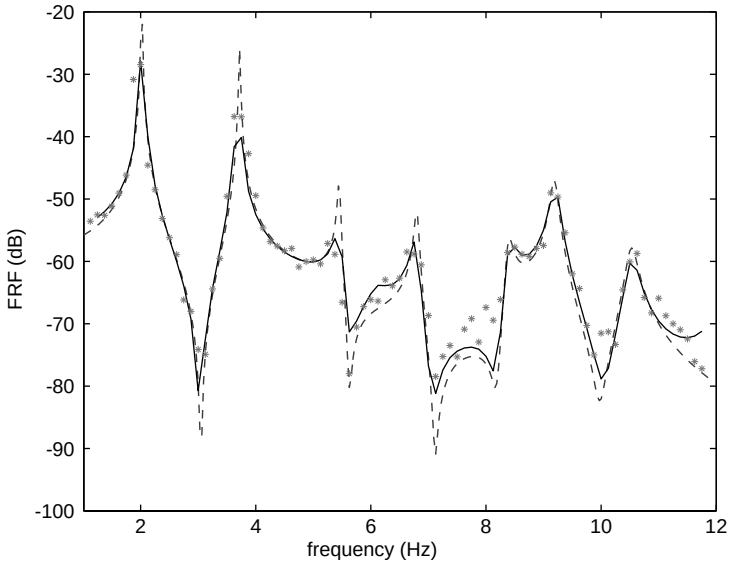

Fig. 5. Synthesized FRF $H_{65}(\omega)$: - - - dashed, exact FRF; $**$, H_1 estimation; ——, MLE-FRF.

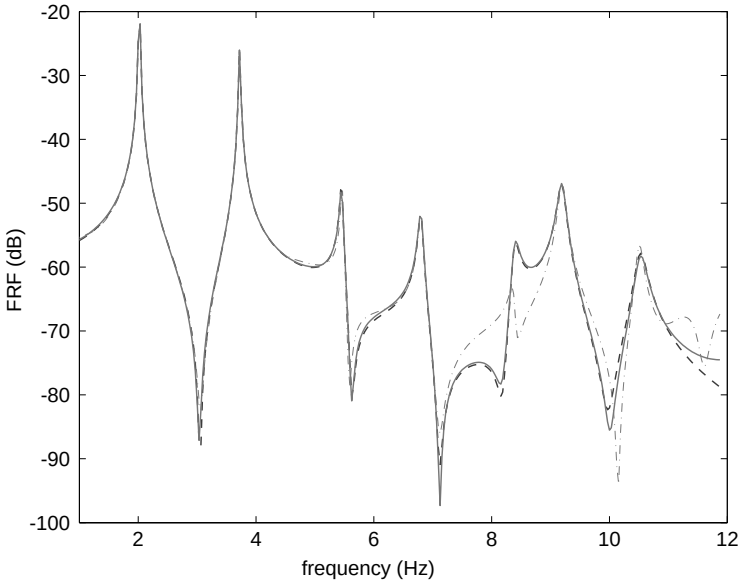

Fig. 6. Synthesized FRF $H_{65}(\omega)$: - - -, exact FRF; ——, CLSF-IO; · – · – ·, MLE-IO.

forces is between 15% and 20%, depending on the output, of the contribution due to the known force. Table 2 draws a comparison between the results obtained by the different estimators. Figs. 7 and 8 show the synthesized FRF H_{65}. Although the standard deviation of the damping ratios are larger than in the previous case, the CLSF-IO method leads to much better results than

Table 2
Overview of modal parameter estimators—combined approach

f_{exact} (Hz)	$m_{f\ CLSF-IO}$ (Hz)	$\sigma_{f\ CLSF-IO}$ (Hz)	$m_{f\ mle\ io}$ (Hz)	$\sigma_{f\ mle\ io}$ (Hz)	$m_{f\ mle\ frf}$ (Hz)	$\sigma_{f\ mle\ frf}$ (Hz)
2.02	2.02	0.001	2.02	0.002	2.01	0.036
3.72	3.72	0.002	3.72	0.004	3.71	0.024
5.45	5.45	0.008	5.46	0.012	5.45	0.039
6.80	6.80	0.003	6.80	0.004	6.80	0.019
8.39	8.39	0.014	8.36	0.036	8.39	0.055
9.19	9.19	0.007	9.20	0.013	9.19	0.020
10.52	10.53	0.009	10.52	0.016	10.52	0.020

d_{exact} (%)	$m_{d\ CLSF-IO}$ (%)	$\sigma_{d\ CLSF-IO}$ (%)	$m_{d\ mle\ io}$ (%)	$\sigma_{d\ mle\ io}$ (%)	$m_{d\ mle\ frf}$ (%)	$\sigma_{d\ mle\ frf}$ (%)
0.16	0.17	0.066	0.15	0.098	0.93	1.337
0.32	0.32	0.066	0.29	0.113	0.87	0.624
0.46	0.46	0.159	−0.03	0.38	1.00	0.804
0.54	0.54	0.035	0.50	0.071	0.91	0.292
0.72	0.71	0.177	−0.63	0.716	1.07	0.710
0.68	0.67	0.074	0.32	0.290	1.06	0.262
0.95	0.94	0.092	0.64	0.263	1.28	0.199

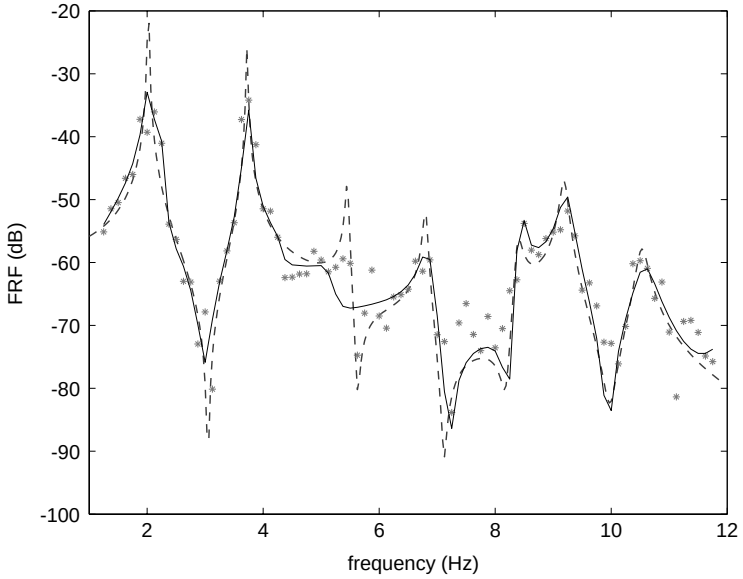

Fig. 7. Synthesized FRF $H_{65}(\omega)$: - - -, exact FRF; $***$, H_1 estimation; ——, MLE-FRF.

the other methods. This simulation approximates aircraft in-flight flutter tests, where the input (e.g., electrical signal to the flaps) and the acceleration measurements are disturbed by atmospheric turbulence (unknown forces). Since the flutter prediction and the determination of

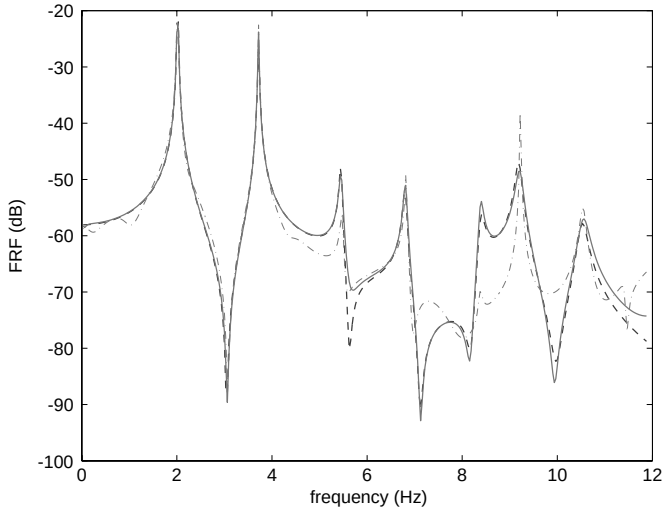

Fig. 8. Synthesized FRF $H_{65}(\omega)$: - - -, exact FRF; ——, CLSF-IO; – · –·, MLE-IO.

Table 3
Overview of modal parameter estimators—output-only approach

f_{exact} (Hz)	$m_{f\ CLSF-IO}$ (Hz)	$\sigma_{f\ CLSF-IO}$ (Hz)	$m_{f\ mle\ frf}$ (Hz)	$\sigma_{f\ mle\ frf}$ (Hz)
2.02	2.02	0.007	2.00	0.015
3.72	3.72	0.011	3.73	0.02
5.45	5.45	0.016	5.45	0.021
6.80	6.80	0.019	6.80	0.026
8.39	8.39	0.033	8.39	0.052
9.19	9.19	0.026	9.18	0.04
10.52	10.53	0.037	10.53	0.054
d_{exact} (%)	$m_{d\ CLSF-IO}$ (%)	$\sigma_{d\ CLSF-IO}$ (%)	$m_{d\ mle\ frf}$ (%)	$\sigma_{d\ mle\ frf}$ (%)
0.16	0.28	0.360	0.06	0.578
0.32	0.44	0.331	0.39	0.612
0.46	0.51	0.296	0.88	0.574
0.54	0.59	0.275	0.72	0.518
0.72	0.75	0.308	0.73	1.142
0.68	0.69	0.259	1.07	0.370
0.95	0.96	0.310	1.34	0.466

the flight envelope of the airplane is based on the estimated damping ratios the obtained results of the CLSF-IO method are promising. The typical overestimation of the damping ratios in case of an H_1 and thus the Hanning window-based method leads to dangerous situations in the prediction of flutter phenomena.

3.3. Case III: operational modal analysis

In this case exactly the same data as in the previous Section 3.2 is processed as output-only data. The output time records were divided into 4 blocks to calculate the spectral density $N_o \times N_o$ matrix $\mathbf{S}_{yy}$. These spectral densities are processed with the MLE FRF method according to Eq. (5). These results are compared to the CLSF-IO method, which operates directly on the output spectra. All the estimates of the natural frequencies and damping are collected in Table 3. The standard deviations of the estimated parameters increased, but the CLSF-IO method still performs much better than the spectral density-based method. Like expected the CLSF-IO method results in more accurate estimates if the measurable forces are taken into account.

4. Experiments

The acoustically excited aluminium plate (see Fig. 9) was measured in 39 points with a scanning laser vibrometer. The structure is excited by two independent loudspeakers. The first loudspeaker is producing periodic noise (each period contains 8192 time samples) to obtain leakage free measurements as a reference. The electric signal to this speaker is measured and used as the known input to the system. The second loudspeaker is connected with a random noise generator. This excitation is an unknown noise source.

During the first test, only the first loudspeaker produces a periodic excitation force on the plate. The responses of 10 periods are averaged with the H_1 estimator to obtain the FRFs. These FRFs

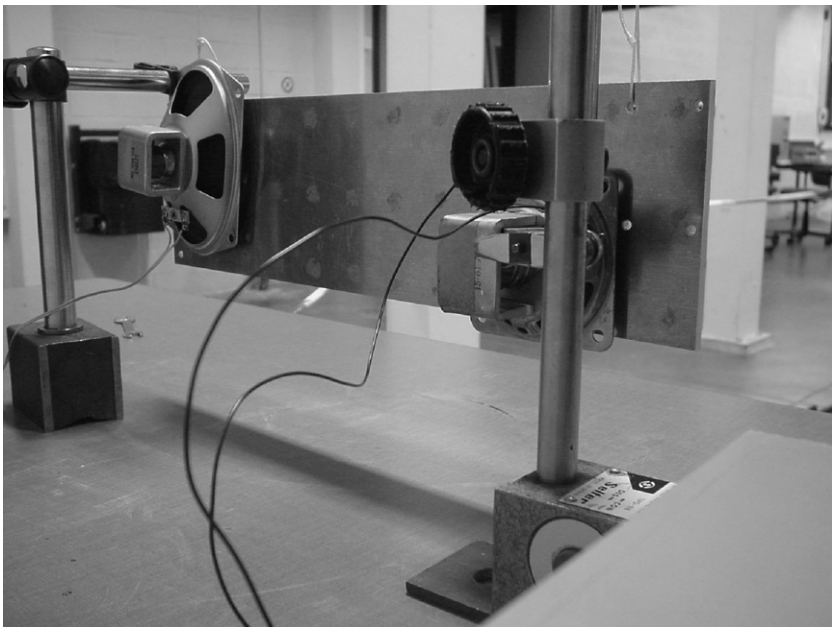

Fig. 9. Experimental set-up.

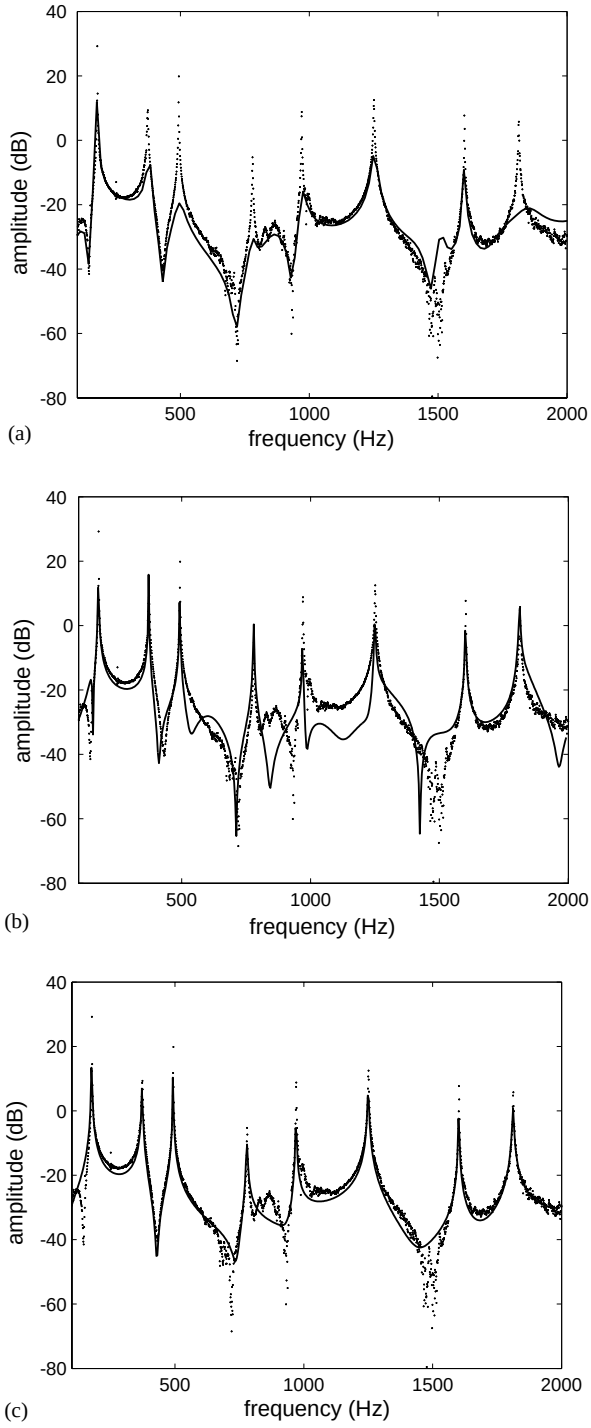

Fig. 10. (a) MLE-FRF, (b) MLE-IO, (c) CLSF-IO; ——, synthesized FRF (2048 samples); ..., measured FRF (8192×10 samples).

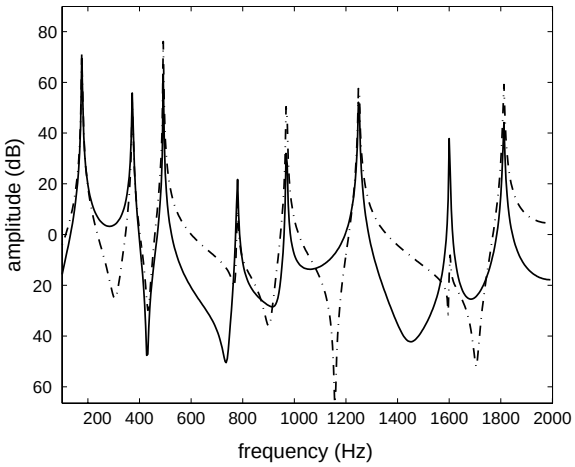

Fig. 11. Deterministic contribution versus stochastic contribution: ——, $H_4\sigma_F$; – · –·, $G_4\sigma_{E_4}$.

are considered as the exact FRFs since no transient (leakage) effects and process noise (unknown forces) disturb the measurements.

During the second test the second loudspeaker is switched on to produce unknown forces simultaneously with the measured forces (first loudspeaker). Only 2048 time samples (a quarter of a period) are measured to obtain the modal model in a frequency band from 100 to 2000 Hz with the MLE FRF, MLE-IO and CLSF-IO methods. Since a sample rate of 2^{13} Hz is used, a maximum frequency resolution of 4 Hz is obtained. This resolution is reached by the IO-based methods, since they work directly on the Fourier spectra of the total time records. The MLE FRF starts from FRFs with a resolution of 16 Hz, since four blocks were used in the averaging process. Fig. 10 illustrates a synthesized FRF by the three identification methods. It is clear that the FRF-based MLE overestimates the damping values due to the transient and leakage effects, while the MLE-IO method suffers from the high level of process noise. The modal model obtained by the CLSF-IO method leads to the best synthesize of the "exact" FRF, Fig. 11. The comparison between the deterministic contribution $H_4(k)\sigma_F$ and the stochastic contribution $G_4(k)\sigma_{E_4}$ in Fig. 11 indicates that the effect of the unknown forces is of the same level as the known forces. In a next step these unknown forces can be located and identified [14].

5. Conclusions

In this paper, the CLSF-IO estimator was presented to process short data sets. This technique can handle leakage effects and unknown forces which operate on the structure. The applicability of this technique was tested by means of Monte Carlo simulations and experiments on a plate. A comparison with existing identification methods, showed that the CLSF-IO gives more accurate results to process short time records in the case of an experimental, operational and combination experimental–operational modal analysis.

Acknowledgements

This research has been supported by the Fund for Scientific Research-Flanders (Belgium) (FWO), the Institute for the Promotion of Innovation by Science and Technology in Flanders (IWT) and by the Research Council (OZR) of the Vrije Universiteit Brussel (VUB).

References

[1] B. Peeters, G. De Roeck, Stochastic system identification for operational modal analysis: a review, Journal of Dynamic Systems, Measurements, and Control 123 (2001) 659–666.
[2] P. Guillaume, P. Verboven, S. Vanlanduit, Frequency-domain maximum likelihood identification of modal parameters with confidence intervals, in: Proceedings of the 23rd International Seminar on Modal Analysis, Leuven, Belgium, September 1998.
[3] G. Dimitriadis, J.E. Cooper, Flutter prediction from flight flutter test data, Journal of Aircraft 38 (2) (2001) 355–367.
[4] A.P. Burrows, J.R. Wright, Optimal excitation for aircraft flutter testing, Journal of Airospace Engineering 209 (1995) 313–325.
[5] W. Johnson, N.K. Gupta, Instrumental variables algorithm for modal parameter identification in flutter testing, American Institute of Aeronautics and Astronautics Journal 16 (8) (1978) 800–806.
[6] J.K. Pinkelman, S.M. Batill, M.W. Kehoe, Total least-squares criteria in parameter identification for flight flutter testing, Journal of Aircraft 33 (4) (1996) 784–792.
[7] P. Verboven, P. Guillaume, M. Van Overmeire, Improved modal parameter estimation using exponential windowing and non-parametric instrumental variables techniques, in: Proceedings of the 18th International Modal Analysis Conference, San Antonio, TX, February 2000.
[8] L. Hermans, H. Van der Auweraer, P. Guillaume, A frequency-domain maximum likelihood approach for the extraction of modal parameters from output-only data, in: Proceedings of the 23rd International Seminar on Modal Analysis, Leuven, Belgium, September 1998.
[9] R. Pintelon, J. Schoukens, System Identification, A Frequency Domain Approach, IEEE Press, New York, 2001.
[10] R. Pintelon, J. Schoukens, G. Vandersteen, Frequency domain system identification using arbitrary signals, IEEE Transactions on Automatic Control 43 (12) (1997) 1717–1720.
[11] R. Pintelon, J. Schoukens, Time series analysis in the frequency domain, IEEE Transactions on Signal Processing 47 (1) (1999) 206–210.
[12] W. Heylen, S. Lammens, P. Sas, Modal Analysis Theory and Testing, K.U. Leuven, Leuven, 1998.
[13] P. Verboven, Frequency-domain System Identification for Modal Analysis, Ph.D. Thesis, Vrije Universiteit Brussel, Departement of Mechanical Engineering, Brussels, 2002.
[14] E. Parloo, P. Verboven, P. Guillaume, M. Van Overmeire, Force identification by means of in-operation modal models, Journal of Sound and Vibration 262 (1) (2003) 161–173.